Available online at www.sciencedirect.com
ScienceDirect
Scripta Materialia 61 (2009) 104–107
Scripta MATERIALIA
www.elsevier.com/locate/scriptamat

Microstructural characterization and isothermal oxidation behavior of hot-pressed TiB_2–10 wt.% $TiSi_2$ composite

G.B. Raju, K. Biswas and B. Basu*

Laboratory for Advanced Ceramics, Department of Materials and Metallurgical Engineering, Indian Institute of Technology, Kanpur 208016, India

Received 12 January 2009; revised 11 March 2009; accepted 11 March 2009
Available online 20 March 2009

This paper reports on the results of fine-scale microstructural characterization and isothermal oxidation of hot-pressed TiB_2–10 wt.% $TiSi_2$ composite. The careful analysis of selected-area diffraction patterns using transmission electron microscopy confirms the presence of Ti_5Si_3 as a reaction product along with TiB_2 and $TiSi_2$ phases. The results of oxidation testing at 1200 °C for 12 h using a thermogravimetric analyzer illustrate near-parabolic oxidation scale growth characteristics. The oxidation mechanisms are discussed with reference to thermodynamically feasible oxidation reactions.

Keywords: TiB_2; Microstructure; Oxidation; TGA

In the last two decades, structural ceramics, in particular, have received wider attention owing to the growing need for high-performance materials in aerospace, automotive sectors and recently for high-temperature applications [1–7]. Among various high-temperature ceramics, titanium diboride (TiB_2) is one of the important materials, belonging to the class of transition metal borides. TiB_2 is characterized by a very good combination of properties, including a relatively high melting point (3225 °C), hardness, high-specific strength, excellent electrical and thermal properties, and good corrosion and wear resistance [8,9].

In fact, for high-temperature structural applications, TiB_2 reinforced with the non-metallic sinter additives is preferred in view of its better properties. Nevertheless, it is very important to understand whether such additives are desirable as far as the high-temperature oxidation properties of TiB_2 are concerned. In general, the oxidation behavior of non-oxide ceramics like TiB_2 largely depends on the composition and properties of the oxidation products [10]. Modification of the chemical composition of the oxide layer is one of the important methods of controlling the oxidation of the ceramics. Recently, numerous studies have reported an improvement in the oxidation resistance of transition metal borides reinforced with 10–30 vol.% of ceramic additives (such as SiC, Si_3N_4, $MoSi_2$, etc.), which are Si sources [10–16]. The oxidation resistance of these ceramics can be improved as a result of the formation of a protective borosilicate glass surface layer.

In an earlier study, investigation revealed that TiB_2 could be densified to >99% of theoretical density (ρ_{th}) with the use of $TiSi_2$ up to 10 wt.% [17]. In continuation of research efforts to realize high-temperature applications of the ceramics developed, an attempt has been made to study the finer-scale microstructure and oxidation resistance of TiB_2 reinforced with $TiSi_2$. The isothermal oxidation of the TiB_2 composite, performed at 1200 °C for 12 h using a thermogravimetric analyzer (TGA) is also reported.

In order to prepare TiB_2–10 wt.% $TiSi_2$ composition, appropriate amounts of commercial TiB_2 (Grade F, H.C. Starck GmbH and Co., Goslar, Germany) and $TiSi_2$ (Goodfellow Cambridge Limited, UK) powders were mixed by wet ball-milling for 12 h in a polyethylene bottle, using SiC balls and ethanol as media. The hot-pressing experiments were carried out at a temperature of 1650 °C for 1 h, with an applied pressure of 30 MPa and a heating rate of 15 °C min^{-1} in a flowing argon gas atmosphere. More details on the starting powders, hot pressing and density measurement are reported elsewhere [17].

The crystalline phases in the starting powders and hot-pressed sample were analyzed by X-ray diffraction

* Corresponding author. Tel.: +91 512 2597771; fax: +91 512 2597505; e-mail: bikram@iitk.ac.in

1359-6462/$ - see front matter © 2009 Acta Materialia Inc. Published by Elsevier Ltd. All rights reserved.
doi:10.1016/j.scriptamat.2009.03.027

(XRD) using Cu K_α radiation. The microstructural investigation of the phase assemblages of the samples was performed by transmission electron microscopy (TEM). TEM observations were performed using a 200 kV Technai G^2 T-20 UTWIN TEM (FEI, Eindhoven, Netherlands), equipped with a high-angle annular dark field (HAADF) detector.

For oxidation experiments, $3 \times 4 \times 10$ mm ceramic coupons were cut using electrodischarge machining (EDM) from the hot-pressed discs. After belt grinding, the samples were polished with diamond paste up to 0.25 μm finish and finally polished with γ-Al_2O_3 (0.05 μm). Prior to the oxidation tests, the polished samples were ultrasonically cleaned in acetone for 10 min and dried at 80 °C overnight. The oxidation tests were carried out at 1200 °C for 12 h in a dry air atmosphere with a heating rate of 30 °C min^{-1}, followed by free cooling. At least two samples from each composition were used. The weight gains were continuously recorded with 10^{-3} mg accuracy, using a TGA (mod. STA409, NETZSCH Gertebau GmbH, Germany) equipped with a vertically heated Al_2O_3 chamber. The samples were placed on platinum supports to separate them from the Al_2O_3 holder. The surface and subsurface of the oxidized samples were analyzed using XRD and scanning electron microscopy (SEM; Quanta model and SIRION model) attached with energy-dispersive spectroscopy (EDS; Oxford Instruments ultrathin window EDS facility) and X-ray mapping to assess the oxide products and to observe the surface morphology of the oxide scales.

The TiB_2–10 wt.% $TiSi_2$ could be densified to >99% ρ_{th} after hot pressing the samples at 1650 °C for 1 h. XRD analysis of the starting powder composition reveals the presence of TiB_2 and $TiSi_2$ phases, while the hot-pressed sample consists of an additional Ti_5Si_3 secondary phase along with the TiB_2 and $TiSi_2$ (Fig. 1a and b). The presence of a new phase (Ti_5Si_3) suggests the involvement of sintering reactions during the hot pressing of TiB_2–$TiSi_2$ material. The details of thermodynamically favorable sintering reactions and sintering mechanisms are beyond the scope of the present paper and are reported elsewhere [17]. In Figure 1c, a HAADF TEM image shows the existence of three contrasting phases in the TiB_2–10 wt.% $TiSi_2$. The phases are marked on the figure. The morphology of TiB_2 grains is either spherical or platelet, and the average grain size of TiB_2 varies between 2 and 3 μm. The size of the Ti_5Si_3 grains ranges from 100 to 150 nm. The microstructure of the sample typically represents bimodal grain morphology with a small fraction of coarser elongated TiB_2 grains along with finer TiB_2 grains, which corroborates the liquid phase sintering (LPS) microstructure. A bright field conventional TEM image of the sample consisting of various microstructural phases is shown in Figure 1d. The Ti_5Si_3 phase is observed to be located at the triple pocket and surrounded by the TiB_2 and $TiSi_2$ grains. The selected-area diffraction patterns (SADP) from various grains confirm the TiB_2 with HCP structure, $TiSi_2$ with orthorhombic structure, and Ti_5Si_3 with HCP structure. The morphology and size of Ti_5Si_3 grains at the triple points of the TiB_2 and $TiSi_2$ is a clear signature of LPS. An important feature of the sintered microstructure is the dislocation activity in some of the TiB_2 grains.

Figure 2 is a bright field image showing a TiB_2 grain with dislocation activity. The presence of dislocations was also reported for the TiB_2–TiC system [18]. Ting and Lu attributed the enhanced densification of $MgAl_2O_4$ spinel to the dislocation substructure [19,20]. The dislocations can act as a short-circuit diffusion path for mass transport during sintering. Hence it is believed that the dislocation activity within the TiB_2 grains in addition to the LPS enhances the sinterability of TiB_2.

Figure 3a shows the variation in weight gain ΔW per unit surface area S as a function of temperature T. In order to compare the oxidation behavior of the TiB_2–$TiSi_2$ composite with the monolithic TiB_2, the weight gain data of monolithic TiB_2 (densified to 96% ρ_{th} after hot pressing at 1800 °C for 1 h) are also presented in Figure 3a and b. The details of hot pressing, microstructure and oxidation behavior of monolithic TiB_2 are reported elsewhere [21]. It can be noted here that the weight gain of the TiB_2–10 wt.% $TiSi_2$ composite is relatively lower than that of the monolithic TiB_2. In general, for both the TiB_2 samples the weight gain shows an increasing trend with temperature. At ~500 °C, the oxidation of the sample is started, and a very slow mass gain is noticed up to 750 °C. Such slow oxidation kinetics is mainly due to the formation of molten B_2O_3, which acts as a protective layer and inhibits the diffusion of oxygen. However, the increase in temperature to 1000 °C causes a sharp increase in the oxidation of the sample, and this is attributed to a rapid increase in the evaporation rate of B_2O_3. It has been widely reported that oxidation starts at ~400–500 °C for the monolithic TiB_2, and the oxidation process is governed mainly by a diffusion mechanism up to 900 °C [22–24]. The oxidation of TiB_2 depends on either the inward diffusion of oxygen ions or the outward diffusion of metal ions into the surface. At high temperatures, borosilicate glass forms, and it hinders the oxygen diffusion and slows down the oxidation kinetics of TiB_2–10 wt.% $TiSi_2$. Hence the diffu-

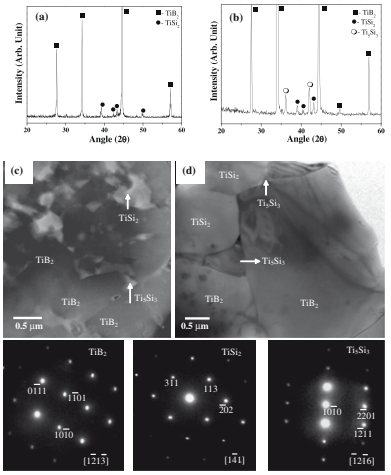

Figure 1. XRD patterns recorded with (a) the starting powder TiB_2–10 wt.% $TiSi_2$ composition and (b) the hot-pressed TiB_2–10 wt.% $TiSi_2$ composite. (c) HAADF TEM image reveals various contrasting phases in the hot-pressed sample. (d) Conventional TEM BF image showing the grain morphology of the various constituent phases. The corresponding SADP were taken from TiB_2, $TiSi_2$ and Ti_5Si_3 phases.